Broadband (kHz–GHz) characterization of instabilities in Hall thruster inside a metallic vacuum chamber

V. Mazières, F. Gaboriau, A. Guglielmi, V. Laquerbe, R. Pascaud, O. Pascal

Broadband (kHz−GHz) characterization of instabilities in Hall thruster inside a metallic vacuum chamber

V. Mazières,[1] F. Gaboriau,[2] A. Guglielmi,[3] V. Laquerbe,[4] R. Pascaud,[1] and O. Pascal[2]
[1)] *ISAE-SUPAERO, 10 Avenue Edouard Belin, 31055 Toulouse, France*
[2)] *LAPLACE, Université de Toulouse, CNRS, INPT, UPS, 118 route de Narbonne, 31062 Toulouse, France*
[3)] *Exotrail, Massy, 91300, France*
[4)] *Antenna Department, Centre National d'Etudes Spatiales (CNES), 31400 Toulouse, France*

(*Electronic mail: valentin.mazieres@isae-supaero.fr)

(Dated: June 24, 2022)

Hall thrusters are known to exhibit a large variety of instabilities. Their physical mechanisms have been identified at low (kHz) and intermediate (MHz) frequencies, even though they are still not fully understood. Furthermore, electromagnetic radiations generated by Hall thrusters, named "self-emission" of the thruster, have been measured from kHz to MHz as expected from the identified instabilities, but also at higher frequencies. The origin of the high frequency (GHz) self-emission remains for now unknown. Assessing this self-emission, that is important for understanding the physics of Hall thrusters as well as for electromagnetic compatibility issues with the spacecraft, is challenging. Another aspect that makes the understanding of the physics of Hall thrusters complex comes from the eventual coupling between instabilities, which has been recently suggested and observed. The aim of this paper is to explore the possibility of characterizing simultaneously instabilities in Hall thrusters on a broadband frequency range (form kHz to GHz) "in-situ", meaning in conventionally used vacuum chamber where Hall thrusters are usually operated. We show in this paper that, despite the reverberant nature of the vacuum metallic chamber, useful information is extracted at low and intermediate frequencies and even at high frequency from the measurements done with an antenna in this environment.

I. INTRODUCTION

In the field of electrical propulsion, Hall thruster (HT) have been widely used and studied over the past decades. These $E \times B$ discharges have shown to be the site of numerous instabilities, *i.e.* collective movement of charged particles. The presence of these instabilities may have a strong influence on the thruster operation and performances[1]. The physical mechanisms behind these instabilities are not perfectly understood nor quantified[2–4]. As a consequence, their contribution to the electron transport referred to as "anomalous" is far to be fully understood and a complete description of this anomalous transport has not yet been found[5]. So far instabilities ranging from kHz to MHz have been identified and widely studied[2–4]. The main instabilities that have been identified are[2–4,6]:

- At low frequency (kHz frequency range):
  - 10–20 kHz: axial "*Breathing mode*" (BM) oscillations, due to the periodic ionization of the atom flux in the region of large magnetic field[7,8].
  - $\sim$ kHz: azimuthal "*Rotating spokes*" (RS) oscillations, which are azimuthal low frequency oscillations[9–11].
  - 100–500 kHz: axial "*Transit time oscillations*" (TTO), due to the propagation of acoustic waves[12,13].
- At intermediate frequency (MHz frequency range):
  - 1–100 MHz: "$E \times B$ *electron drift*" instabilities (EDI), which are azimuthal, small wavelength oscillations[14,15].

These instabilities are gathered in Table I. A review on the instabilities that have been experimentally observed has been done in 2001 by Choueiri[16]. However, further work is still needed on each of these instabilities as their mechanisms and their influence on thruster performances are not well understood. For example, the effects of the presence of the breathing mode on thruster performances is still under discussion[1].

	kHz	MHz	GHz
Known instabilities			
Breathing mode	✓	✗	✗
Rotating spokes	✓	✗	✗
Transit time oscillations	✓	✗	✗
$E \times B$ electron drift instability	✗	✓	✗
Self-emission in EMC test facilities	✓	✓	✓

Table I. Frequencies of the known instabilities and of the measured self-emission in EMC test facilities of Hall thrusters.

Hall thruster instabilities consist in azimuthal or axial oscillations or acceleration of charged particles. As a consequence, electromagnetic radiation at these frequencies will occur, which can be referred to as "self-emission" of the thruster. This radiation can act as a source of electromagnetic noise for the spacecraft. Measurements of the self-emission of HT have been made to check and validate the electromagnetic compatibility (EMC) between the thruster and the spacecraft. This self-emission of HT have been measured these past decades in particular by Beiting *et al*[17–22] and Kirdyashev[23,24]. Hall thrusters have been shown to radiate electromagnetic waves ranging from kHz to GHz, as represented in Table I. The GHz radiation does not correspond to any known instability

and an accurate description of its physical origin is still required. In a paper of 1999[6], it is highlighted that for plasma densities of about $10^{10} - 10^{11}$ cm^{-3}, the plasma frequency (or Langmuir frequency) fall into the GHz range. The GHz radiations measured experimentally may thus be a consequence of the oscillations of electrons in the plasma thruster. For the GHz radiation measured in a more recent paper[18], the author also explained this radiation by the oscillation of electrons at the plasma frequency. Other work from Kirdyashev have suggested that this GHz self-emission emanates from the cathode[23], which is consistent with the results of Beiting *et al*[18]. In a more recent paper of Kirdyashev[24], the cathode is also found to be the main source of GHz oscillations and a physical model of a thruster as a source of GHz radiations is proposed. However, more work is required to confirm or refute all of these hypotheses. The physical origin of these electron oscillations and their link with the thruster operating principles remain for now unknown. In addition to being important for EMC issues, measurement of the thruster self-emission could be a useful tool for characterizing electrical thruster, and in particular HT. Indeed, a lot of useful information about the physical phenomena that occur inside the plasma thruster is contained in its self-emission.

Hence, instabilities in HT occur from kHz frequencies up to at least GHz frequencies. Furthermore, recent works have shown that coupling between these instabilities may occur. For example, coupling between BM and RS instabilities may be possible and has been reported[1,25–27] and coupling between low (kHz) and intermediate (MHz) frequencies has also recently been suggested[27,28]. In the recent paper of Kirdyashev[24], it is even envisioned that the microwave oscillations (GHz) in the thruster acceleration channel may be one of factors governing anomalous transverse plasma conductivity. Understanding the coupling between instabilities is essential as "in any real HT, anomalous electron transport may be the result of the complex interaction between a number of different instabilities."[28]. This coupling is also of particular importance for improving the thruster performances, as it suggests the possibility of driving these instabilities. This has been done recently, for example by applying external modulations of the applied voltage[1,29]. This external modulation allows the control of the breathing mode oscillations, and it has been shown that it allows the suppressing of the breathing mode as well as the rotating spokes[1].

Several difficulties are encountered when trying to evaluate the coupling between these instabilities. The main one comes from the need to be able to simultaneously measure them. Usually, investigations of instabilities have been done at low frequency (kHz) using for example Faraday probes[30], cameras[31–33] or Langmuir probes[34–36] and at intermediate frequency (MHz) using for example collective light scattering[14,37], electrically small antennas inserted in the dense regions of the plasma plume[38–41] or Langmuir probe[34–36]. For the high frequency (GHz) instabilities, the fast variations of the field that need to be captured by the measuring system makes this evaluation particularly complex. One way to do it would be to measure the self-emission resulting from these high frequency (GHz) instabilities. However, it cannot be characterized in conventional anechoic chambers, since the thruster must be operated in vacuum. Thus, dedicated test facilities have been implemented, consisting in the coupling of an anechoic chamber and a metallic vacuum chamber, with the aim of avoiding any interaction of the waves with metallic walls during electromagnetic measurements. We will refer to them in this paper as “EMC test facilities” to differentiate them from the common test facilities that are used for characterizing Hall thruster by other diagnostics. These EMC test facilities are sparse, bulky, and expensive and to the best of our knowledge, only three of this kind of facilities have been built: the one of Aerospazio in Italy[42], of the Aerospace Corporation in USA[43] and of the RIAME facility in Russia[44]. To circumvent this problem of evaluating high frequency instabilities, Kirdyashev proposed recently to use microwave probes inserted directly into the dense region of the plasma plume (at a few centimeters away from the anode), allowing local measurement of these microwave instabilities[24]. In this case, a precise evaluation of the influence of the presence of the dense plasma around the probe on its frequency behavior needs to be conducted[24]. The significant difference of time and space scales of these instabilities, ranging from kHz to GHz, as well as their difference of physical nature, makes their simultaneous evaluation complex. A similar difficulty is found in numerical simulations of HT. For example, the modeling of the breathing and azimuthal spoke modes has usually been performed separately[25] and the high frequency (GHz) instabilities have not yet been found in simulation. More work on the simultaneous evaluation of instabilities in HT is thus required.

The aim of this paper is to explore the possibility of characterizing simultaneously instabilities in HT on a broadband frequency range (form kHz to GHz) "in-situ", meaning in commonly used test facility, that consists in metallic vacuum chambers. The idea is to put an electrically small antenna inside the vacuum chamber, far away from the dense regions of the plasma plume. Then, by analyzing the behavior of the waves inside cavity, we show in this paper that it is possible to extract useful information from the measurements. It results in the identification of the operating modes of the thruster in frequency ranges corresponding to known instabilities (from kHz to MHz). At higher frequencies (GHz), to our knowledge it leads to the first identification of the operating modes of the thruster from measurements done in metallic test facility.

This article is organized as follows: in section II, the ID-Hall thruster and facilities are briefly described and we present the electric sensor used for the electromagnetic characterization of the Hall thruster in the metallic vacuum chamber. The procedure used to extract valuable information from the measurements is presented. In section III, we characterize with the sensor the ID-Hall Thruster by varying the discharge voltage and we make a broadband analysis of the signal that we link with common instabilities encountered in Hall thruster.

II. EXPERIMENTAL SETUP

A. Thruster and test facility

The ID-Hall thruster (for Inductive Double stage) is a double stage Hall thruster where the ionization stage is a magnetized RF inductively coupled plasma source with an RF coil inside the inner cylinder of the thruster, with the aim of increasing the plasma density before its acceleration[30,45]. A schematic of the ID-Hall design and its magnetic field is shown in Figure 1. The assembly of inductive coil (of the ICP source), ferrite, and magnets is contained inside a 26 mm diameter Pyrex tube, which is also the inner wall of the thruster. The outer wall is made of alumina, and it can be divided in a cylindrical channel with a diameter of 46 mm and a length of 10 mm, and a conical ionization chamber (of the ICP source) with a length of 30 mm and an outer wall with an increasing diameter up to 92 mm and the base of the cone.

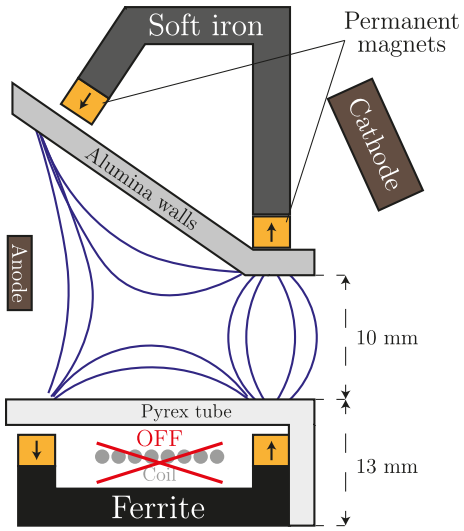

Figure 1. Schematic of the ID-Hall thruster prototype used in this study, showing a schematic of the magnetic field lines. In this study, the ID-Hall thurster is used in "single stage operation", meaning the ICP source is not powered.

In this study, the ID-Hall thruster is used in “single stage operation”, *i.e.* there is no additional power from the ICP source (in other word the ICP source is not powered, as shown in Figure 1) and the thruster operation is similar to the classical Hall thruster operation. This thruster was fixed at one end of a cylindrical vacuum vessel with a length of 1 m and a diameter of 0.5 m[30,46]. The vessel is equipped with three turbomolecular pumps, providing a total pumping speed of 5650 l/s once the transparency of the protection grids is taken into account. All measurements presented here were performed with a Xenon flow of 6 sccm through the anode side and 1.5 sccm through the cathode; under these conditions, the background pressure was 6×10^{-5} mbar. The ensemble of anode, cathode, and starter/keeper together with their power sources are floating with respect to the grounded chamber walls. The discharge voltage, corresponding to the difference of the potential between anode and cathode, will be varied form 110V to 350V. All of the measurements presented in this paper have been obtained within a few minutes following the ignition of the thruster.

The method deployed in this paper consists in putting an electrical sensor inside the metallic vacuum chamber, as represented in Figure 2. The signal $r(t)$ measured by the sensor is recorded with a Keysight MSO9254A oscilloscope, which has a bandwidth of $f_{max} = 4$ GHz and a sample rate of 20 GS/s.

B. Design of the electrical sensor

From an electromagnetic point of view, the emission of a signal $e(t)$ at a certain location inside of the cavity leads to a signal $r(t)$ collected by the sensor, which is a convolution of $e(t)$ and the impulse response $h(t)$ of the system, composed of the sensor and the vacuum chamber. Assuming that the presence of the sensor does not have a significant influence on the cavity response (dimension of the sensor small compared to the cavity dimensions), $h(t)$ can be expressed as $h(t) = h_c(t) * h_s(t)$, with $h_c(t)$ the impulse response of the cavity and $h_s(t)$ the impulse response of the sensor. In the frequency domain, this is equivalent to say that

$$R(f) = E(f).H_c(f).H_s(f) \tag{1}$$

with $R(f)$, $E(f)$, $H_c(f)$ and $H_s(f)$ the Fourier transforms of $r(t)$, $e(t)$, $h_c(t)$ and $h_s(t)$, respectively.

From equation (1) we can see that the measured signal $R(f)$ results in a product of the emitted signal $E(f)$ with two transfer functions $H_c(f)$ and $H_s(f)$, corresponding to the cavity and the sensor respectively. The transfer function of the cavity $H_c(f)$ reflects the behavior of the waves inside the cavity between the location of their emission and the location of the sensor. At certain frequencies, namely the resonant frequencies, a resonance phenomenon occurs that generates “peaks” on the magnitude of $H_c(f)$ at these frequencies. The frequency of the first resonant mode (meaning the one with the lowest frequency), named “fundamental frequency”, depends on the cavity volume, shape (and losses). For our reverberant cavity, this fundamental frequency f_f is approximately equal to 380 MHz.

In order to mitigate the influence of the measuring system on the measured signal, the electrical sensor should have a flat frequency transfer function $H_s(f)$ on the useful $[0:4]$ GHz bandwidth, so that the sensor do not have a significant influence on the waveform of $r(t)$. An easy way to obtain such a flat response consists in using an electrically small antenna. Thus, the antenna is designed so that its first resonant frequency f_f^a is greater than 4 GHz. Finally this antenna consists of a metallic conductor of about 1 cm, acting as a monopole, with a fundamental frequency of about $f_f^a \sim 10$ GHz. Because of its small dimension as compared to the wavelengths associated with the frequencies of the useful bandwidth, the sensitivity of this antenna is low, in the sense that it does not behave as an efficient antenna. A picture of this antenna is shown in Figure 2.

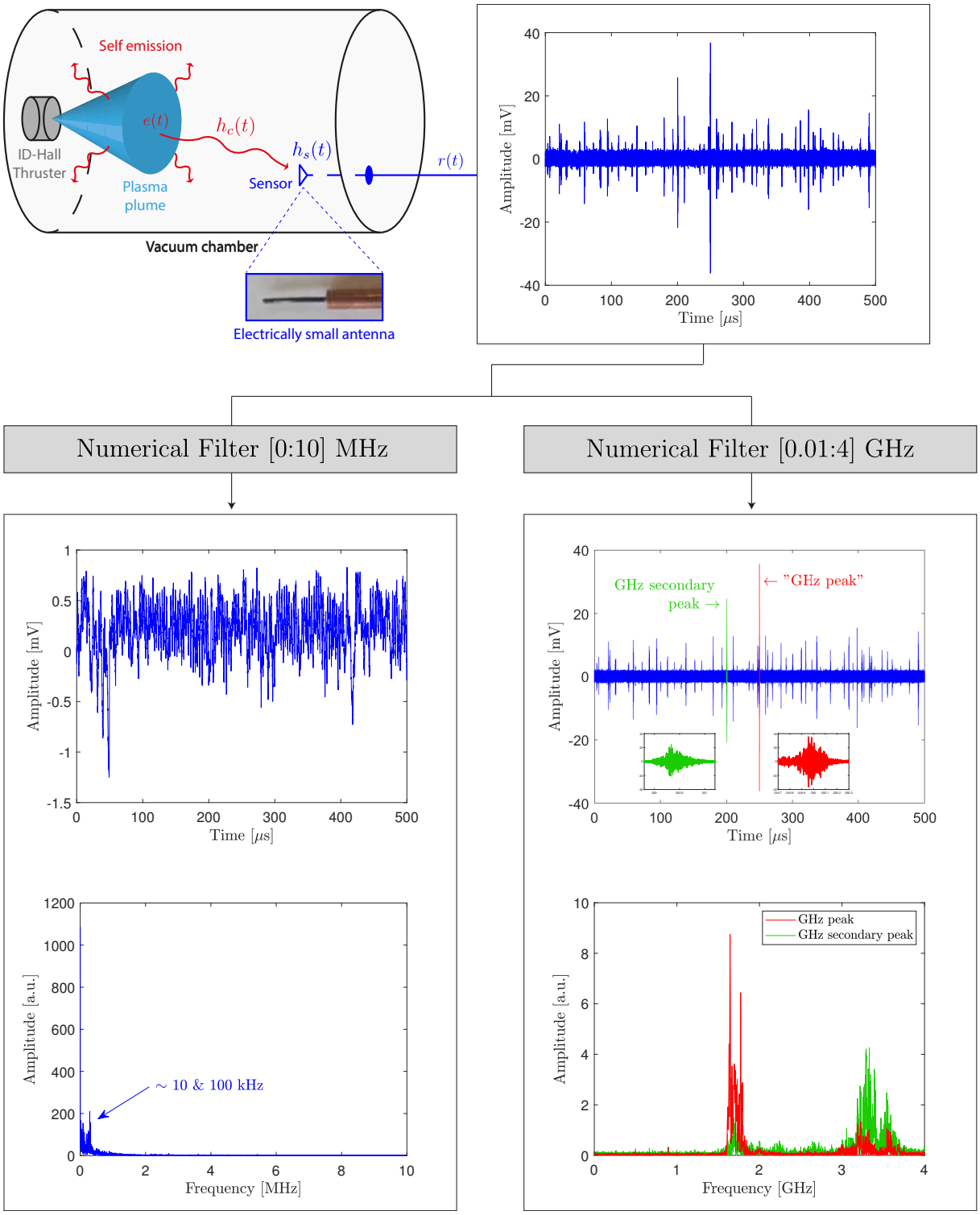

Figure 2. Example of a measurement with a discharge voltage of 150 V.

Electrically small antennas have already been used for investigating MHz instabilities of Hall thrusters[38–41]. However, these antennas protruded into the discharge area of the thruster, at 2 mm from the channel exit[39]. Hence, particular attention should be made for these antennas to operate in this harsh environment[41]. In this configuration, the signal measured by the antennas has been said to come from a capacitive coupling between the antenna and the thruster[39].

In our case, the antenna is fixed inside the metallic cavity at a distance of about 80 cm away from the thruster, offset from the central axis of the thruster. Since the antenna is far from the dense regions of the plasma plume, we can legitimately

assume that the plasma density is very low at the antenna location and hence its transfer function $H_s(f)$ should not be affected by the eventual presence of charged particles.

C. Information captured by the antenna

Self-emission of Hall thrusters have been measured in EMC test facilities from kHz up to GHz frequencies[17–24]. And as it is shown in this paper, information is also captured from kHz up to GHz frequencies by using the antenna described before. However, the nature of the mechanism by which this information is captured depends on the frequency. Two frequency ranges can be distinguished when analyzing the signal measured by the antenna.

For frequencies lower than the fundamental frequency f_f of the resonant cavity, the dimensions of the cavity are lower than the wavelength of the waves. As a consequence, no propagating wave can exist in the cavity at these frequencies. However, as it is shown in this paper, information is still measured by the antenna. From an electromagnetic point of view, in this frequency range (for $f < f_f$), the cavity behaves as a waveguide excited below its cut-off frequency[47]. Hence, the fields in the cavity follow spatially an exponential decay and the magnitude of its transfer function $H_c(f)$ smoothly increases with frequency, up to f_f (there is no intensification since there is no resonance phenomenon). As a first approximation, this transfer function can thus be assumed to be constant on relatively narrow frequency ranges. From a signal point of view, the measured signal is an accurate image of the corresponding instability (on a certain narrow frequency band).

For frequencies higher than the fundamental frequency f_f of the resonant cavity, the dimensions of the cavity are bigger than the wavelength of the waves. As a consequence, standing waves can exist in the cavity. Any instabilities oscillating in this frequency range will radiate waves that can propagate in the cavity, and that can be captured by the antenna. The measured signal $r(t)$ is thus significantly modified by the cavity transfer function $H_c(f)$. It is largely enhanced by a resonance phenomenon at the cavity resonance frequencies. In this case the measured signal $r(t)$ is the result of wave propagation and reflection due to the emission of $e(t)$ in the cavity.

Thus, the nature of the mechanism by which the antenna capture information is certainly different for these two frequency ranges, meaning a non-radiative coupling for $f < f_f$ and a radiative coupling for $f > f_f$.

Note that in addition to these possible couplings, the capture of information by the antenna could also come from a local coupling due to the presence of moving charged particles at the antenna location, even if the plasma density is low at this location. In this case the mechanism of capture of information is similar to the one consisting in putting a probe into the dense regions of the plasma plume. Furthermore the presence of a plasma inside of the cavity can affect, depending on its density and dimensions, the spectral behavior of the transfer function $H_c(f)$. For example, its fundamental frequency f_f can be shifted due to the presence of the plasma. More work is planned in the future on these effects.

Finally, the information captured by the antenna could depend on its location inside of the vacuum chamber and of its polarization. However, for the results showed in this paper, several locations and polarizations have been tested and yielded similar results in term of global trends. For more details about this investigation see Supplementary materials. Hence, in our experimental set-up, the location and polarization of the antenna do not seem to have a significant impact on the trends and interpretations proposed in this paper (from the results obtained with one antenna).

D. Example of a measured signal

An example of a signal $r(t)$ measured with a discharge voltage of 150 V is plotted on Figure 2. There is a lot of information contained in this signal. To extract this information, ideal numerical filters are first applied to this signal. One that focuses on the low frequency (kHz) and intermediate frequency (MHz) range and the other one that focuses on the high frequency (GHz) range.

On the left side of Figure 2, the filtered signal with the low frequency numerical filter is plotted versus time and frequency. For this operating point, the measured signal does not exhibit any significant intermediate (MHz) frequency components. Its most significant frequency components are the continuous component and the ones of about 10 and 100 kHz, which correspond respectively to breathing mode and/or rotating spokes and transient time instabilities.

On the right side of Figure 2, the filtered signal with the high frequency numerical filter is plotted in blue in the time domain. It is organized in pulses of duration of about a few hundred of nanoseconds (it is important to note though that part of this duration is a consequence of the storage of the electromagnetic energy in the cavity and its reverberation time is around 100 ns), that all have frequency components between about 1 and 4 GHz. For example, in the insets, the pulse with the highest amplitude − that we name "GHz peak" − and another pulse − that we name "GHz secondary peak" − are plotted in red and green, respectively. They are also represented in the frequency domain on the bottom figure. Their most significant frequency components are concentrated around 1.7 and 3.4 GHz. These frequency components are organized in narrow frequency peaks, that correspond to the resonant frequencies of the cavity. We see here the influence of the presence of the metallic cavity on the measured signal (because the maximal frequency of the filter is higher than f_f).

E. Temporal average of the "GHz peak"

As it has been observed for other Hall thrusters on measurements that have been done in EMC test facilities[19,22], the behavior of the self-emission of the ID-Hall thruster in the GHz frequency range has a random nature that complicates its characterization. In order to analyze this GHz self-emission, statistical analyses have been implemented. They consist in

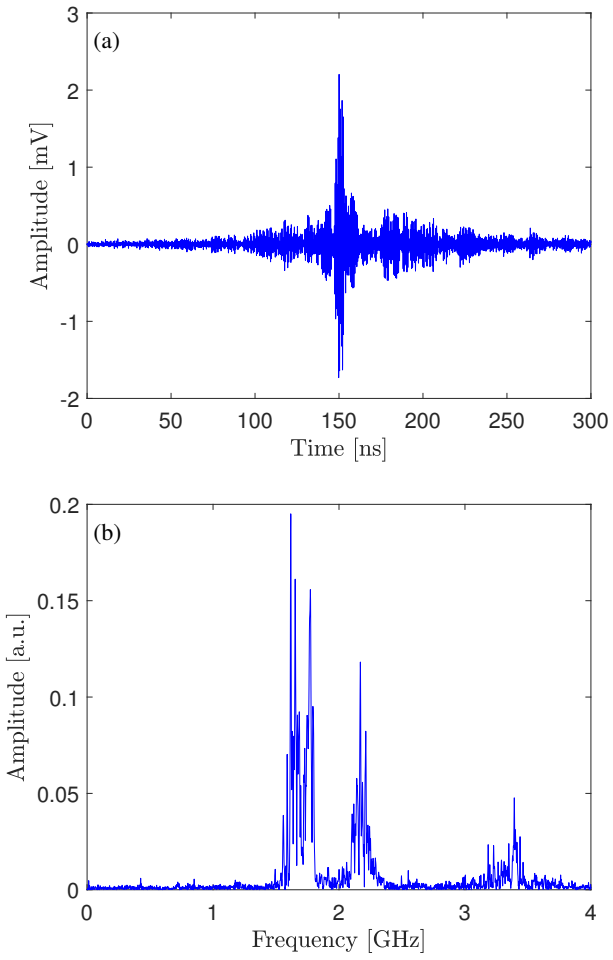

Figure 3. Average of the "GHz peak" for a discharge voltage of 150 V. (a) In the time domain. (b) In the frequency domain.

investigating the duration, frequency components, and amplitude of these GHz pulses for different operating points. This has been shown to allow to extract some trends about the behavior of theses GHz pulses, depending on the operating conditions. However, this statistical analysis requires to process a certain amount of data sets to be effective.

For the HT under study, although the GHz self-emission has a random nature, there is always a pulse with a high amplitude, the "GHz peak", surrounded by pulses with lower amplitudes, as can be seen for example on Figure 2. In order to characterize this GHz self-emission, we propose in this paper to focus on the temporal average of these "GHz peaks". In practice, the level of the oscilloscope trigger is adjusted to trigger on the GHz peak and a temporal average is done by the oscilloscope (on a few thousands of measurements). For example, the temporal averaged signal and its frequency spectrum for a discharge voltage of 150 V are plotted on Figure 3[48]. The main interest of this temporal average is that it allows to handle reproducible signals. In other words, for each operating conditions of the thruster corresponds an unique GHz averaged signal. This allows us to characterize the GHz self-emission as a function of the discharge voltage, as it is done in the following section.

III. RESULTS AND DISCUSSION

The aim of this section is to show that there is useful information contained in the signals measured in reverberant cavity by an antenna located far away from the dense regions of the plasma plume. To that end, the signals are measured by the antenna described previously for different values of the discharge voltage. Analyzing the evolution of the frequency of the instabilities as a function of the discharge voltage have been shown to be an effective way to identify the operating modes of Hall thrusters[49–52].

A. Identification of the operating modes on the current-voltage curve

The current versus voltage discharge curve is plotted in Figure 4. The evolution of the current is in good agreement with previous characterizations of the ID-Hall thruster in single stage operation for discharge voltages up to 280 V[30]. For discharge voltages between 280 and 350 V, the current had been found to increase with the discharge voltage up to about 0.9 A[30] whereas in the results of the present paper this current decreases from 280 to 300 V, before increasing with the discharge voltage up to about 0.7 A. Note that the reproducibility of this behavior has been checked. The origin of this difference remains unknown, but may come from the wearing of the thruster, and it particular from the wall erosion, which have been shown to have an influence on the thruster performances[53].

On this current-voltage curve, six operating regimes can be identified depending on the evolution of the discharge current as a function of the discharge voltage, as represented on Figure 4. Note that in ref.[30], strong amplitude variations of the discharge current has been found in operation modes from ① to ③.

B. Low frequency (kHz) instabilities

Signals are measured for different discharge voltages. Then a numerical filter (such as the one presented in previous section) between 0 and 100 kHz is applied on those signals. The corresponding frequency components of these signals are plotted in Figure 5 as a function of the discharge voltage. The operating modes that have been identified on the current-discharge characteristic are also reported on this Figure.

In operating regime ①, the frequency of the main component in this part of the spectrum linearly increases with the voltage discharge from about 3 kHz at 110 V up to 9 kHz at 170 V. In previous characterizations based on the current oscillations, it had been found that the breathing mode was present in this frequency range. Its frequency have also been

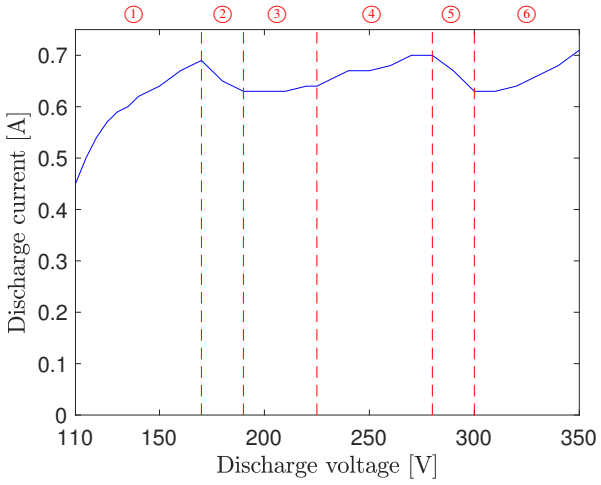

Figure 4. Identification of the operating mode on the curve of the discharge current as a function of the discharge voltage.

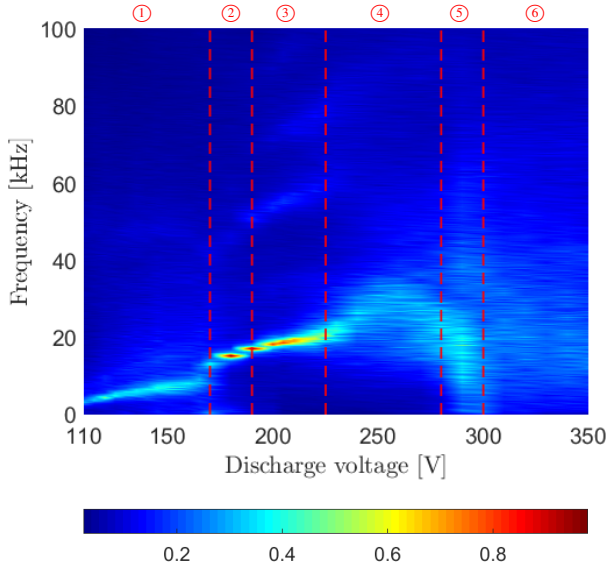

Figure 5. Low frequency ($0-100$ kHz) components as a function of the discharge voltage.

found to increase with the discharge voltage, with slightly higher frequencies (around 10 kHz)[30]. The frequency component measured in this operating regime is thus probably related to the breathing mode.

In operating regime ②, corresponding to a decrease of the discharge current, the principal frequency component does not follow a linear increase with the discharge voltage. We observe a three-steps increase with the discharge voltage, at 13, 15 and 17 kHz. These frequency components are the most intense obtained for the whole voltage range. Although there is clearly a change of regime between operating regimes ① and ②, for discharge voltages below 190 V, breathing mode have been found to be present in previous characterizations, with a frequency increasing with the discharge voltage up to a frequency of 15 kHz at 180 V[30]. This change of regime is also visible on the amplitude of the current oscillations (thought to be the sign of the presence of the breathing mode), as this amplitude have been found to drop significantly from 170 V to 190 V[30]. Thus, this three-steps increase of the principal frequency component may be also due to the breathing mode.

In operating regime ③, the principal frequency component linearly increases with the voltage discharge from about 17 kHz at 190 V up to 20 kHz at 225 V. For discharge voltages higher than 190 V, the breathing mode have been found to disappear, as the current oscillations have been found to be significantly small[30]. Based on these results, the origin of this increasing frequency component from 17 to 20 kHz is probably not due to breathing mode oscillations. It could come from azimuthal rotating spokes, which generally have frequencies in this frequency range. However, these rotating spokes have been found to rather be present at low discharge voltage[6]. In addition, in this operating regime, two secondary frequency components, around 55 and 75 kHz, are also present and increasing with the discharge voltage. The origin of the frequency components of this operating regime remains unknown, and further work should be done to investigate its physical origin.

In operating regimes ④, ⑤ and ⑥ the frequency spectrum spreads over a certain frequency range, reflecting the fact that the physical mechanisms at the origin of these frequency components is less organized, more random than for previous operating modes. For operating regime ④ the spectrum is contained between 10 and 40 kHz, for operating regime ⑤ the spectrum is contained between 0 and 50 kHz and for operating regime ⑥ the spectrum is contained between 5 and 50 kHz.

The results presented in this subsection show that the known frequency instabilities in this frequency range are well captured by the diagnostic proposed in this paper.

C. High frequency (GHz) instabilities

The same procedure as the one used in the previous subsection III B is used for GHz self-emission. In this case the numerical filter, between 0.5 and 4 GHz is applied on the average of the GHz peaks for each discharge voltage. The corresponding frequency components of the self-emission of the ID-Hall thruster are plotted in Figure 6 as a function of the discharge voltage.

First it is important to note that a relative comparison between the levels obtained at low (kHz) and high (GHz) frequencies is not directly possible. Indeed, some of the frequency components that are measured above the fundamental frequency of the cavity – of $f_f = 380$ MHz in our case – have been intensified by the cavity resonances whereas it is not the case for frequencies lower than f_f.

The influence of the presence of resonant modes in this frequency range is visible on the spectrum plotted in Figure 6. For example, around 1 GHz for discharge voltage around 250 V, three main spectrally narrow contributions are visible, certainly corresponding to resonant modes of the cavity.

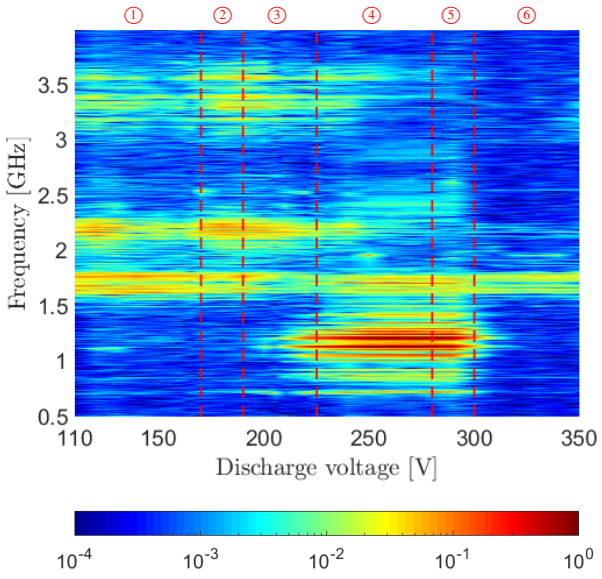

Figure 6. High frequency ($0.5-4$ GHz) average self-emission as a function of the discharge voltage.

A direct relative comparison between the amplitudes components for different frequencies may also not be judicious. Indeed, the transfer function $H(f)$ between the thruster and the antenna is unknown, making the self-emission of the thruster hard to evaluate at these frequencies in metallic cavities. This comparison could maybe be envisioned in an overmoded cavity, as the field inside is statistically isotropic and spatially uniform, which is equivalent to say its spectral behavior is statistically flat. As a first approximation, the frequency above which the cavity becomes overmoded is about 3 or 6 times the fundamental frequency (it corresponds to the "lowest usable frequency")[54]. In our case, this frequency is found around 1.7 GHz. Thus, our cavity can not be considered as overmoded on the useful frequency range (at least not on the whole frequency range). Hence, for the analysis presented in the present paper, this comparison is not done. Another consequence is that the frequency ranges that have been identified for the GHz self-emission (for example around 1 GHz for discharge voltages around 250 V) may be the result of the spectral shape of the transfer function $H(f)$. However, this measurement of the GHz self-emission in reverberant cavity still allows to clearly identify different operating modes.

The operating regimes that have been identified on the current-discharge characteristic are reported on Figure 6. We can see that the characteristics of the GHz self-emission depends on the discharge voltage. At low discharge voltages (below 225 V), the frequencies of the self-emission is distributed into several contributions, around 1.7 GHz, 2.2 GHz and 3.3 GHz. Between 225 V and 300 V the bandwidth of about 400 MHz around 1 GHz corresponds to GHz self-emission. At higher discharge voltages, the frequencies of the self-emission is concentrated around 1.7 GHz. We can see that some of the operating regimes are also found at these high frequencies. For example, the self-emission around 1 GHz is only present in operating regimes ④ and ⑤. Overall, this kind of information is really useful for both physical understanding and EMC concerns.

D. Level of the electric field of the GHz self-emission

Self-emission from the thruster can act as a source of electromagnetic noise for the spacecraft. This is particularly critical as the receivers of spacecraft are designed to be highly sensitive in order to capture relatively small amount of power coming from ground stations (located on Earth). For example, GHz self-emission can be troublesome for satellites that have receiver frequencies in the L (1-2 GHz), S (2-4 GHz), and C (4-8 GHz) bands. Thus, measurements of the self-emission of HT have been made in the EMC test facilities for the verification of the electromagnetic compatibility between the thruster and the spacecraft. Very recently, Kirdyashev studied the disturbance induced by the GHz self-emission on the communication with a spacecraft[55]. In the present subsection, information about the level of the GHz electric field radiated by the ID-Hall thruster is extracted from the measurements done inside the reverberant cavity.

The antenna factor AF of the antenna, linking the measured voltage V_a to the electric field at the antenna, has been evaluated as a rough approximation to be of about $AF \sim 360\ \mathrm{m}^{-1}$ at GHz frequencies. For the different operating conditions studied in this paper, the level of measured voltage V_a of the GHz pulses is of about a few tens of mV, as can be seen for example on Figure 2. Taking $V_a^{max} \sim 50$ mV (which is the maximum voltage value measured for the different operating conditions), the maximal level of the estimated electric field measured by the antenna is of about $E^{max} = AF.V_a^{max} \sim 20$ V/m. The level of this electric field is the result of the filtering of the emitted signal $e(t)$ by the transfer function of the system. Thus it does not correspond to the level of this GHz self-emission emitted in free space, but it could give information about the order of magnitude of this radiated electric field. More work is planned in the future that will focus in a more detailed investigation of the level of this radiated electric field.

E. Broadband (kHz−GHz) analysis

Lastly, a broadband analysis, from kHz to GHz, is conducted. Two frequency ranges, namely $[100:500]$ kHz and $[0.5:10]$ MHz are added to the two previous frequency ranges studied ($[0:100]$ kHz and $[0.5:4]$ GHz). These two added frequency ranges remain inferior to the fundamental frequency of the cavity, so no resonance phenomenon will be present. This broadband characterization of the ID-Hall thruster, along with the corresponding possible instabilities, are plotted on Figure 7. For frequencies lower than the fundamental frequency of the cavity, the plots have been normalized to the highest amplitude found on this frequency range ($[0:10]$ MHz). The plot at high frequency is normalized to the highest amplitude found in this frequency range.

At low frequency (kHz), we find Figure 5 that has been analysed in section III B, with the associate possible sources

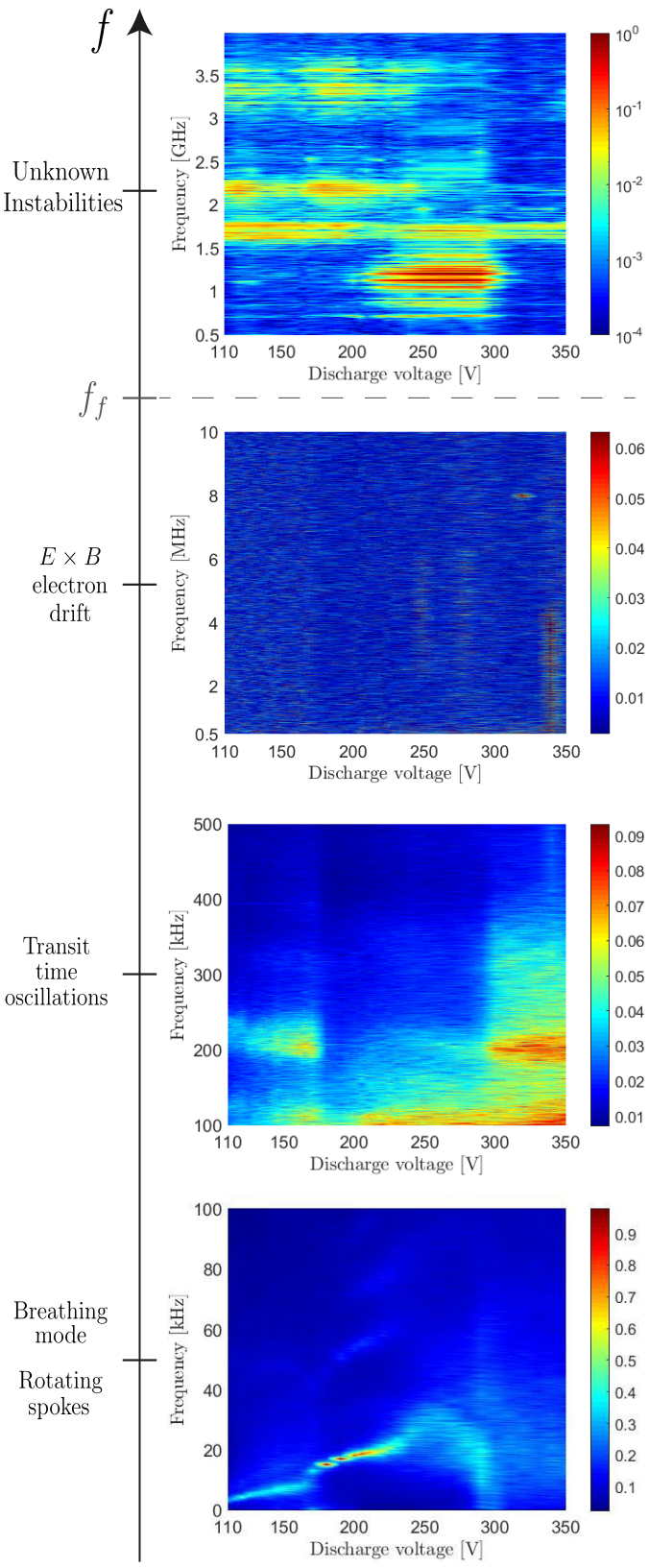

Figure 7. Broadband analysis of the ID-Hall thruster as a function of the discharge voltage, with the corresponding possible instabilities.

of these frequency components: Breathing mode (BM) and Rotating spokes (RS).

At higher frequencies, between 100 kHz and 500 kHz, we find amplitudes that are much lower than the ones of the principal frequency components that have been found between 0 and 100 kHz[56]. A relatively strong contribution is found around 200 kHz for low discharge voltages (below 170 V) and for high discharge voltages (above 300 V), which corresponds to operating regimes ① and ⑥, respectively. The origin of these frequency components could be the transit time oscillation (TTO) that has been found to oscillate at these frequencies.

At intermediate frequencies, between 500 kHz and 10 MHz, the amplitudes found are even lower than for the previous frequency range. The only significant contribution is found in the operating regime ⑥ for a discharge voltage of 340 V. This contribution is found between 400 kHz (on the previous plot) and about 4 MHz. The origin of these frequency components could be the $E \times B$ electron drift instability (EDI) that has been found to oscillate at these frequencies.

At high frequency (GHz), we find Figure 6 that has been analysed in section III C. The physical mechanisms at the origin of this self-emission remains for now unknown.

Globally, the operating modes identified from the current-voltage characteristic seem to be in good agreement with the evolution of the frequency components as a function of the discharge voltage. This shows the ability of the proposed method to investigate simultaneously instabilities of HT on a broadband frequency range.

IV. CONCLUSION

Characterization of the instabilities of the ID-Hall thruster (used in single stage operation) has been done "in-situ", meaning inside the vacuum chamber. It consists in putting an electrically small antenna inside the metallic test facility where the thruster is operated, far away from the dense regions of the plasma plume, and then analyzing the measured signals.

This characterization has been done in the frequency range $[0:4]$ GHz. Frequency components are found around kHz, around $\sim$100 kHz and $\sim$1 MHz, which could be the consequence of known instabilities, meaning breathing mode - rotating spokes, transit time oscillations and $E \times B$ electron drift instability, respectively. Frequency components are also observed in the $[0.5:4]$ GHz frequency range. It is found to possess a random nature. Using the temporal average of the GHz pulse with the highest amplitude, this GHz self-emission has been characterized as a function of the discharge voltage. Different operating regimes are found for the broadband measurements as a function of the discharge voltage, which seem globally to be in good agreements with the operating modes identified on the current-voltage characteristic. In the future, more elaborated analysis should be done to extract even more information of these measurements.

This kind of diagnostic, easy to implement (consisting of a simple antenna put inside commonly used test facilities), could be a handy additional tool for investigating the physics

of HT. Furthermore, it possess features that none of the commonly used diagnostics for characterizing HT have. First, it allows a broadband (from kHz to GHz) characterization, providing a general overview of the mechanisms at play in HT. Instabilities can be simultaneously investigated, which could be really useful for understanding possible coupling between them. Furthermore, for frequencies below the fundamental frequency of the reverberant cavity, the information captured by the antenna is not much affected by the presence of the cavity (in term of spectral behavior). The ability to investigate high frequency (GHz) could really be useful for understanding the origin of the GHz self-emission. Finally, it gives information about the electromagnetic compatibility of the thruster with the spacecraft, which is a question of major interest for small spacecraft, where the thruster and the spacecraft apparatus are closed to each other.

SUPPLEMENTARY MATERIALS

See supplementary materials for insights about the influence of the antenna location and polarization on the results presented in this paper.

ACKNOWLEDGMENTS

This work was supported by the French Space Agency CNES. V. Mazières benefited from a postdoctoral research grant financed by the CNES. The authors are grateful to Alberto Rossi for the support.

REFERENCES

[1] I. Romadanov, Y. Raitses, and A. Smolyakov, "Control of Coherent Structures via External Drive of the Breathing Mode," Plasma Phys. Rep. **45**, 134–146 (2019).

[2] J.-P. Boeuf, "Tutorial: Physics and modeling of Hall thrusters," Journal of Applied Physics **121**, 011101 (2017).

[3] S. Mazouffre, "Electric propulsion for satellites and spacecraft: established technologies and novel approaches," Plasma Sources Sci. Technol. **25**, 033002 (2016).

[4] K. Hara, "An overview of discharge plasma modeling for Hall effect thrusters," Plasma Sources Sci. Technol. **28**, 044001 (2019).

[5] D. A. Tomilin and I. A. Khmelevskoi, "Influence of kinetic effects on long wavelength gradient-drift instability in high-frequency range in Hall thruster," Physics of Plasmas **27**, 102103 (2020).

[6] V. V. Zhurin, H. R. Kaufman, and R. S. Robinson, "Physics of closed drift thrusters," Plasma Sources Sci. Technol. **8**, R1–R20 (1999).

[7] J. P. Boeuf and L. Garrigues, "Low frequency oscillations in a stationary plasma thruster," Journal of Applied Physics **84**, 3541–3554 (1998).

[8] S. Barral and E. Ahedo, "Low-frequency model of breathing oscillations in Hall discharges," Phys. Rev. E **79**, 046401 (2009).

[9] R. Kawashima, K. Hara, and K. Komurasaki, "Numerical analysis of azimuthal rotating spokes in a crossed-field discharge plasma," Plasma Sources Sci. Technol. **27**, 035010 (2018).

[10] E. Rodríguez, V. Skoutnev, Y. Raitses, A. Powis, I. Kaganovich, and A. Smolyakov, "Boundary-induced effect on the spoke-like activity in E × B plasma," Physics of Plasmas **26**, 053503 (2019).

[11] A. I. Morozov, Y. V. Esipchuk, A. M. Kapulkin, V. A. Nevrovskii, and V. A. Smirnov, "Effect of the magnetic field a closed-electron-drift accelerator," Sov. Phys.-Tech. Phys. (Engl. Transl.) 17: No. 3, 482-7(Sep 1972). (1972).

[12] S. Barral, K. Makowski, Z. Peradzyński, and M. Dudeck, "Transit-time instability in Hall thrusters," Physics of Plasmas **12**, 073504 (2005).

[13] J. Vaudolon and S. Mazouffre, "Investigation of the ion transit time instability in a Hall thruster combining time-resolved LIF spectroscopy and analytical calculations," in *51st AIAA/SAE/ASEE Joint Propulsion Conference* (American Institute of Aeronautics and Astronautics, 2015).

[14] S. Tsikata, N. Lemoine, V. Pisarev, and D. M. Grésillon, "Dispersion relations of electron density fluctuations in a Hall thruster plasma, observed by collective light scattering," Physics of Plasmas **16**, 033506 (2009).

[15] J. C. Adam, A. Héron, and G. Laval, "Study of stationary plasma thrusters using two-dimensional fully kinetic simulations," Physics of Plasmas **11**, 295–305 (2004).

[16] E. Y. Choueiri, "Plasma oscillations in Hall thrusters," Physics of Plasmas **8**, 1411–1426 (2001).

[17] E. Beiting, J. Pollard, V. Khayms, and L. Werthman, "Electromagnetic Emission to 60 GHz from a BPT 4000 Edm Hall Thruster," in *28th International Electric Propulsion Conference (IEPC-03-129)* (Toulouse, France, 2003).

[18] E. Beiting, M. Garrett, J. Pollard, and B. Pezet, "Spectral Characteristics of Radiated Emission from SPT-100 Hall Thrusters," in *Proc. 29th International Electric Propulsion Conference (Princeton University), IEPC-2005-221* (2005).

[19] E. J. Beiting, M. L. Garrett, J. E. Pollard, B. Pezet, and P. Gouvernayre, "Temporal Characteristics of Radiated Emission from SPT-100 Hall Thrusters in the L, S, and C Bands," in *29 th International Electric Propulsion Conference, IEPC-2005-222* (Princeton University, 2005).

[20] E. Beiting, M. Garrett, and J. Pollard, "Spectral and Temporal Characteristics of Electromagnetic Emissions from the BPT-4000 Hall Thrusters," in *42nd AIAA/ASME/SAE/ASEE Joint Propulsion Conference & Exhibit* (American Institute of Aeronautics and Astronautics, 2006).

[21] E. Beiting, X. L. Eapen, J. Pollard, and M. Gambon, "Electromagnetic Emissions from PPS ® 1350 Hall Thruster," in *IEPC-2009-071* (2009).

[22] E. Beiting, R. Spektor, and X. Eapen, "Time-Domain Characteristics of 0.2 - 8 GHz Pulsed Emission from Hall Thrusters," in *46th AIAA/ASME/SAE/ASEE Joint Propulsion Conference & Exhibit*, Joint Propulsion Conferences (American Institute of Aeronautics and Astronautics, 2010).

[23] K. P. Kirdyashev, "Electomagnetic interference with hall thruster operation," in *Proc. 4th Int. Spacecraft Propulsion Conf. Cagliari* (Sardinia, Italy, 2004) pp. 307–312.

[24] K. P. Kirdyashev, "Microwave processes in the SPD-ATON stationary plasma thruster," Plasma Phys. Rep. **42**, 859–869 (2016).

[25] I. D. Kaganovich, A. Smolyakov, Y. Raitses, E. Ahedo, I. G. Mikellides, B. Jorns, F. Taccogna, R. Gueroult, S. Tsikata, A. Bourdon, J.-P. Boeuf, M. Keidar, A. T. Powis, M. Merino, M. Cappelli, K. Hara, J. A. Carlsson, N. J. Fisch, P. Chabert, I. Schweigert, T. Lafleur, K. Matyash, A. V. Khrabrov, R. W. Boswell, and A. Fruchtman, "Physics of E x B discharges relevant to plasma propulsion and similar technologies," Physics of Plasmas **27**, 120601 (2020).

[26] K. Matyash and R. Schneider, "3D simulation of rotating spoke in a wallless Hall thruster," in *Proceedings of the 36th International Electric Propulsion Conference* (Vienna, Austria, 2019) pp. Paper No. IEPC–2019– 437.

[27] W. Liqiu, H. Liang, Y. Ziyi, L. Jing, C. Yong, Y. Daren, and D. Jianhua, "Modulating action of low frequency oscillations on high frequency instabilities in Hall thrusters," Journal of Applied Physics **117**, 053301 (2015).

[28] T. Charoy, T. Lafleur, A. A. Laguna, A. Bourdon, and P. Chabert, "The interaction between ion transit-time and electron drift instabilities and their effect on anomalous electron transport in Hall thrusters," Plasma Sources Sci. Technol. **30**, 065017 (2021), publisher: IOP Publishing.

[29] I. Romadanov, Y. Raitses, and A. Smolyakov, "Hall thruster operation with externally driven breathing mode oscillations," **27**, 094006 (2018).

[30] A. Martín Ortega, A. Guglielmi, F. Gaboriau, C. Boniface, and J. P. Boeuf, "Experimental characterization of ID-Hall, a double stage Hall thruster with an inductive ionization stage," Physics of Plasmas **27**, 023518 (2020).

[31] Y. Dancheva, D. Pagano, S. Scaranzin, R. Mercatelli, M. Presi, F. Scortecci, and G. Castellini, "Non-intrusive tools for electric propulsion diagnostics," CEAS Space J (2021), 10.1007/s12567-021-00360-w.

[32] V. Désangles, S. Shcherbanev, T. Charoy, N. Clément, C. Deltel, P. Richard, S. Vincent, P. Chabert, and A. Bourdon, "Fast Camera Analysis of Plasma Instabilities in Hall Effect Thrusters Using a POD Method under Different

Operating Regimes," Atmosphere **11**, 518 (2020).
[33]M. McDonald and A. Gallimore, "Parametric Investigation of the Rotating Spoke Instability in Hall Thrusters," undefined (2011).
[34]R. B. Lobbia and A. D. Gallimore, "High-speed dual Langmuir probe," Review of Scientific Instruments **81**, 073503 (2010).
[35]V. I. Demidov, S. V. Ratynskaia, and K. Rypdal, "Electric probes for plasmas: The link between theory and instrument," Review of Scientific Instruments **73**, 3409–3439 (2002).
[36]A. A. Litvak, Y. Raitses, and N. J. Fisch, "Experimental studies of high-frequency azimuthal waves in Hall thrusters," Physics of Plasmas **11**, 1701–1705 (2004).
[37]S. Tsikata, C. Honoré, N. Lemoine, and D. M. Grésillon, "Three-dimensional structure of electron density fluctuations in the Hall thruster plasma: $\bar{E}\times\bar{B}$ mode," Physics of Plasmas **17**, 112110 (2010).
[38]A. Lazurenko, V. Vial, M. Prioul, and A. Bouchoule, "Experimental investigation of high-frequency drifting perturbations in Hall thrusters," Physics of Plasmas **12**, 013501–013501–9 (2005).
[39]A. Lazurenko, L. Albaréde, and A. Bouchoule, "Physical characterization of high-frequency instabilities in Hall thrusters," Physics of Plasmas **13**, 083503 (2006).
[40]A. Lazurenko, V. Krasnoselskikh, and A. Bouchoule, "Experimental Insights Into High-Frequency Instabilities and Related Anomalous Electron Transport in Hall Thrusters," IEEE Transactions on Plasma Science **36**, 1977–1988 (2008).
[41]A. A. Litvak, Y. Raitses, and N. J. Fisch, "High-frequency probing diagnostic for Hall current plasma thrusters," Review of Scientific Instruments **73**, 2882–2885 (2002).
[42]M. Albani, F. Puggelli, A. Toccafondi, G. Meniconi, and F. Scortecci, "Modeling and dielectric characterization of EMI/EMC ground test for the evaluation of the electric propulsion thruster emissions," in *2017 IEEE International Symposium on Antennas and Propagation USNC/URSI National Radio Science Meeting* (2017) pp. 2599–2600.
[43]E. Beiting, "Design and performance of a facility to measure electromagnetic emissions from electric satellite thrusters," in *37th Joint Propulsion Conference and Exhibit* (American Institute of Aeronautics and Astronautics, Salt Lake City, Utah, 2001).
[44]S. V. Baranov, N. Vazhenin, A. Plokhikh, G. Popov, Y. V. Kochev, Y. Ermoshkin, and A. V. Pervukhin, "Determination of Electromagnetic Emission from Electric Propulsion Thrusters under Ground Conditions IEPC-2017-167," in *35th International Electric Propulsion Conference* (Georgia Institute of Technology - Atlanta, Georgia - USA, 2017).
[45]L. Dubois, F. Gaboriau, L. Liard, D. Harribey, C. Henaux, L. Garrigues, G. J. H. Hagelaar, S. Mazouffre, C. Boniface, and J. P. Boeuf, "ID-HALL, a new double stage Hall thruster design. I. Principle and hybrid model of ID-HALL," Physics of Plasmas **25**, 093503 (2018).
[46]F. Diop, T. Gibert, and A. Bouchoule, "Argon ionization improvement in a plasma thruster induced by few percent of xenon," Physics of Plasmas **26**, 063508 (2019).
[47]D. Russell, "The waveguide below-cutoff attenuation standard," IEEE Transactions on Microwave Theory and Techniques **45**, 2408–2413 (1997), conference Name: IEEE Transactions on Microwave Theory and Techniques.
[48]Note that frequency components around 2.2 GHz, that were not present in the frequency content of the GHz peak plotted on Figure 2, are found on the temporal average on those GHz peaks in these conditions (discharge voltage of 150V).
[49]N. Gascon, M. Dudeck, and S. Barral, "Wall material effects in stationary plasma thrusters. I. Parametric studies of an SPT-100," Physics of Plasmas **10**, 4123–4136 (2003).
[50]L. Wei, C. Wang, C. Zhang, and D. Yu, "Effects of operating parameters on ionization distribution in Hall thrusters," Appl. Phys. Lett. **102**, 173505 (2013).
[51]E. Chesta, C. M. Lam, N. B. Meezan, D. P. Schmidt, and M. A. Cappelli, "A characterization of plasma fluctuations within a Hall discharge," IEEE Transactions on Plasma Science **29**, 582–591 (2001).
[52]N. Gascon, C. Perot, S. Bechu, P. Lasgorceix, B. Izrar, M. Dudeck, G. Bonhomme, and X. Caron, "Signal processing and non-linear behavior of a Stationary Plasma Thruster - First results," in *35th Joint Propulsion Conference and Exhibit* (American Institute of Aeronautics and Astronautics, 1992).
[53]N. P. Brown and M. L. R. Walker, "Review of Plasma-Induced Hall Thruster Erosion," Applied Sciences **10**, 3775 (2020).
[54]D. A. Hill, "Electromagnetic Theory of Reverberation Chambers," **1506** (1998).
[55]K. P. Kirdyashev, "The electromagnetic problems of interplanetary spacecraft communication," **1560**, 012077 (2020).
[56]The fact that the frequency component around 100 kHz seems to be of high intensity on this plot whereas it seemed not to be present on the plot below ($[0:100]$ kHz) comes from the change of scale between those plots.